

Journal of Mathematical Extension
Vol. 15, No. 4, (2021) (11)1-16
URL: <https://doi.org/10.30495/JME.2021.1724>
ISSN: 1735-8299
Original Research Paper

An Extended Element Free Galerkin Method Based on Moving Kriging Interpolation for Second-Order Elliptic Interface Problems

A. Taleei

Shiraz University of Technology

Abstract. The aim of this paper is to introduce an efficient meshless element free Galerkin technique for solving elliptic interface problems. In this work, the second-order elliptic equation with discontinuous coefficients and homogeneous and nonhomogeneous jump conditions is considered. Moving kriging interpolation is chosen to construct shape functions in the proposed method. To apply the jump conditions in the weak form of the problem, Nitsche's method is used. Some examples are presented to confirm the effectiveness of the proposed method for interface problems.

AMS Subject Classification: MSC: 82B24 ; 35J05; 35J57.

Keywords and Phrases: Meshless method; Element free Galerkin (EFG); Moving kriging interpolation (MKI); Nitsche's method.

1 Introduction

In three past decades, considerable attention has been paid to meshless numerical methods, due to their flexibility in solving boundary value problems [24]. Meshless methods are created to eliminate part of the

Received: June 2020; Accepted: August 2020

difficulties associated with reliance on a mesh to construct the approximation [3]. In these methods, the approximation of unknown in the partial differential equation is constructed based on scattered points while no mesh is needed in the construction of their approximation [6]. Several meshless methods, such as the element free Galerkin (EFG) method [6], the finite point (FP) method [20], the finite cloud (FC) method [2] the moving least-squares reproducing kernel (MLSRK) method [26], the meshless local Petrov Galerkin (MLPG) method [3] have been introduced and achieved significant progress in solving a wide class of boundary value problems.

Many important physical and industrial applications involve mathematical models with a very complicated structure that is characterized by discontinuous or even singular material properties. These problems are known as interface problems. Interface problems arise in various branches of science and engineering. These problems usually lead to differential equations whose input data and solutions are nonsmooth or discontinuous across some interfaces [21]. Recently, a variety of meshless methods have been applied to second-order elliptic problems with the closed interface (see [1, 8, 14, 18, 28, 29, 30, 35] and the references therein).

The EFG method [6] is one of the most famous meshless methods based on the weak form that the discrete equation is obtained by the Galerkin method [6, 7, 11, 27]. Nowadays, the EFG method has been developed to be a formidable competitor and also a beneficial complement to the traditional finite element method, which has dominated engineering analysis [25, 33, 34]. However, one of the disadvantages of the EFG method based on moving least-squares approximation is the enforcement of the Dirichlet boundary condition due to the lack of Kronecker delta property of the moving least-squares approximation [15, 23]. An effective way to solve this problem is to use the moving kriging interpolation (MKI) instead of the moving least-squares approximation in the EFG method [15]. The EFG method based on MKI has been studied to solve a variety of PDEs (see [9, 32] and the references therein). The MKI possesses the Kronecker delta function property and enables the EFG method to impose the Dirichlet boundary condition directly [31, 34]. For more information on the properties of MKI, interested readers can

see [15].

In the meshless methods based on MKI, the smoothness of the shape function is determined by that of the basis functions, and the correlation functions. However, the employment of smooth approximation near interface leads to a difficulty in handling problems with discontinuities in the solution or its derivatives. To obtain accurate discontinuous solutions using meshless methods, several different approaches have been proposed [5, 19, 24]. An efficient and simple technique is the visibility criterion scheme that the support domain of the shape function or approximation function is cut by the interface. This technique leads to a proper approximation near the closed interface problems [28].

The Lagrange multipliers method, the penalty method, and Nitsche's method are three common approaches for enforcing jump conditions in numerical methods based on weak form (see [13] and the references therein). Note that these techniques are also used to apply Dirichlet conditions in the meshless weak form methods based on approximations that do not have the Kronecker delta function property [18, 25]. As said in [13], the use of the Lagrange multipliers leads to additional unknowns and a mixed method is get. Jannesari and Tatari proposed the EFG method based on the moving least-squares approximation for the elliptic interface problem. They used the Lagrange multipliers to enforce both Dirichlet boundary condition and Dirichlet jump condition [18]. In the penalty method, no additional unknowns obtain, but the conditioning of the coefficient matrix scales with the order of the penalty parameter that enforces the constraint [25]. Nitsche's method can be considered as a consistent penalty method [12]. Therefore, this method does not contain additional unknowns, and also the conditioning of the coefficients matrix is not largely affected by a stabilization parameter [16].

In this work, the study of the EFG method based on MKI is proposed for the closed interface boundary value problems. The visibility criterion method is chosen for the production of discontinuous shape functions at the near interface. This technique, by truncating the support of the correlation function, ignores the nodes on the other side of the interface. As in a closed interface, the influence domain of the shape function or approximation function is completely cut by a discontinuity, then this choice is proper. Also, this modification of correlation function possesses

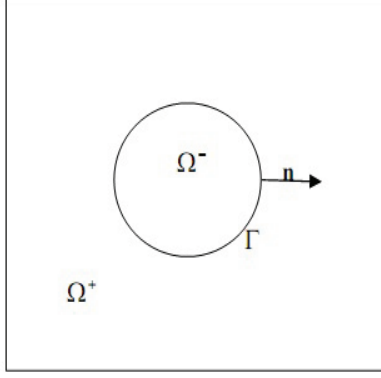


Figure 1: A rectangular domain Ω with the interface Γ .

simplicity since the computational domain splits into two sub-domains that in each domain, a boundary value problem with a smooth solution is solved [29]. To impose the jump conditions in the weak form of the problem, Nitsche's method is used.

The rest of the paper is organized as follows: Section 2, introduces the interface problem used in this work and presents the variational formulation for the studied interface problem by using Nitsche's method. In Section 3, the extended EFG method based on MKI with correlation modification is described for the interface problem. Some examples are presented to show the performance of the proposed technique in Section 4. Finally, a conclusion is given in Section 5.

2 Mathematical formulation

Let Ω be a convex domain with Lipschitz continuous boundary in \mathbb{R}^2 , which is separated into two disjoint subregions Ω^+ and Ω^- by an interface Γ , i.e. $\Omega = \Omega^+ \cup \Omega^- \cup \Gamma$, where Γ is a closed interface. Thus it does not pass the origin within the domain (see Figure 1 for a geometric illustration). Also, the vector $\mathbf{n} = (n_x, n_y)$ be the unit normal direction of Γ pointing from the Ω^- phase to the Ω^+ phase or pointing outward to

the boundary. Consider the two-dimensional elliptic equation as follows

$$-\nabla \cdot (\kappa \nabla u) + \beta u = f, \quad \text{in } \Omega^+ \cup \Omega^-, \quad (1)$$

with the boundary conditions:

$$u(\mathbf{x}) = g_D(\mathbf{x}), \quad \text{on } \partial\Omega_D, \quad (2)$$

$$\kappa \nabla u(\mathbf{x}) \cdot \mathbf{n} = g_N(\mathbf{x}), \quad \text{on } \partial\Omega_N, \quad (3)$$

and the jump conditions on the interface Γ :

$$[u]_\Gamma(\mathbf{x}) \equiv u^+(\mathbf{x}) - u^-(\mathbf{x}) = g_1(\mathbf{x}), \quad \text{on } \Gamma, \quad (4)$$

$$\left[\kappa \frac{\partial u}{\partial \mathbf{n}} \right]_\Gamma(\mathbf{x}) \equiv \kappa^+ \frac{\partial u^+}{\partial \mathbf{n}}(\mathbf{x}) - \kappa^- \frac{\partial u^-}{\partial \mathbf{n}}(\mathbf{x}) = g_2(\mathbf{x}), \quad \text{on } \Gamma. \quad (5)$$

The coefficients κ, β , and the source term f may be discontinuous across the interface Γ . It should be noted that u^+ and u^- are used to denote the limiting values of the field u as the interface is approached from either Ω^+ or Ω^- , respectively. The weak form of the interface boundary value problem (1)-(5) is:

$$\text{Find } u \in \mathcal{U} \text{ such that } a(u, v) = l(v) \quad \forall v \in \mathcal{V},$$

$$\begin{aligned} a(u, v) = & \int_{\Omega} (\kappa \nabla u \cdot \nabla v + \beta uv) d\Omega \\ & + \int_{\Gamma} (-\{\kappa \nabla u \cdot \mathbf{n}\} [v]_\Gamma - [u]_\Gamma \{\kappa \nabla v \cdot \mathbf{n}\} + \alpha [u]_\Gamma [v]_\Gamma) ds, \end{aligned} \quad (6)$$

$$l(v) = \int_{\Omega} f v d\Omega + \int_{\partial\Omega_N} g_N v ds + \int_{\Gamma} (\alpha g_1 [v]_\Gamma - g_1 \{\kappa \nabla v \cdot \mathbf{n}\} + g_2 \{v\}) ds. \quad (7)$$

$\mathcal{U} = \{u | u \in H^1(\Omega^+ \cup \Omega^-), u = g_D(\mathbf{x}) \text{ on } \partial\Omega_D\}$ and $\mathcal{V} = \{v | v \in H^1(\Omega^+ \cup \Omega^-), v = 0 \text{ on } \partial\Omega_D\}$ are the trial and test spaces, respectively. Here, $\{\cdot\}$ denotes the average quantity on the interface Γ such that $\{u\} = \frac{1}{2}(u^+ + u^-)$.

3 Numerical method

Since the MKI as the trial and test functions are chosen in the global weak form of the model, a brief review of this method is given, firstly. To modify the approximation near the interface, the modification of correlation function is applied, therefore the visibility criterion technique is introduced [6]. At last, a system of discretized equations corresponding to the studied boundary value problem is obtained.

3.1 MKI scheme

The MKI scheme is generally considered to be one of the schemes to approximate data with reasonable accuracy. Here we give a summary of the MK interpolation. For more details of the MKI, see [31]. Consider a set of nodes scattered in a domain Ω and \mathbf{x}_i be the coordinates of node i . Let the local approximation $u^h(\mathbf{x})$ of $u(\mathbf{x})$ in a small neighbourhood $\Omega_{\mathbf{x}}$ of \mathbf{x} be as follows

$$u^h(\mathbf{x}) = \mathbf{\Phi}(\mathbf{x})\mathbf{u}, \quad \mathbf{x} \in \Omega_{\mathbf{x}}, \quad (8)$$

where $\mathbf{\Phi}(\mathbf{x}) = [\phi_1(\mathbf{x}), \dots, \phi_n(\mathbf{x})]$, and $\mathbf{u} = [u_1, u_2, \dots, u_n]^T$ is a vector of nodal variables. The shape function $\mathbf{\Phi}(\mathbf{x})$ of MKI is defined as [15]

$$\mathbf{\Phi}(\mathbf{x}) = \mathbf{p}(\mathbf{x})\mathcal{A} + \mathbf{r}(\mathbf{x})\mathcal{B}, \quad (9)$$

where $\mathbf{p}(\mathbf{x}) = [p_1(\mathbf{x}), p_2(\mathbf{x}), \dots, p_m(\mathbf{x})]$, $p_j(\mathbf{x})(j=1,2,\dots,m)$ are monomial basis functions, m is the number of terms of the basis. $\mathbf{r}(\mathbf{x})$ is the vector of correlation function between point \mathbf{x} and the given local nodes which are located inside the supporting domain of \mathbf{x} ,

$$\mathbf{r}(\mathbf{x}) = [\rho(\mathbf{x}, \mathbf{x}_1), \rho(\mathbf{x}, \mathbf{x}_2), \dots, \rho(\mathbf{x}, \mathbf{x}_n)].$$

The matrices \mathcal{A} and \mathcal{B} are the following forms

$$\mathcal{A} = (\mathcal{P}^T \mathcal{R}^{-1} \mathcal{P})^{-1} \mathcal{P}^T \mathcal{R}^{-1},$$

$$\mathcal{B} = \mathcal{R}^{-1} (I - \mathcal{P} \mathcal{A}),$$

where \mathcal{P} is the $n \times m$ matrix that has the polynomial basis function values at the given nodes

$$\mathcal{P} = \begin{bmatrix} p_1(\mathbf{x}_1) & \dots & p_m(\mathbf{x}_1) \\ p_1(\mathbf{x}_2) & \dots & p_m(\mathbf{x}_2) \\ \dots & \ddots & \vdots \\ p_1(\mathbf{x}_n) & \dots & p_m(\mathbf{x}_n) \end{bmatrix},$$

and \mathcal{R} is the $n \times n$ symmetric correlation matrix as follows

$$\mathcal{R} = \begin{bmatrix} \rho(\mathbf{x}_1, \mathbf{x}_1) & \dots & \rho(\mathbf{x}_1, \mathbf{x}_n) \\ \rho(\mathbf{x}_2, \mathbf{x}_1) & \dots & \rho(\mathbf{x}_2, \mathbf{x}_n) \\ \dots & \ddots & \vdots \\ \rho(\mathbf{x}_n, \mathbf{x}_1) & \dots & \rho(\mathbf{x}_n, \mathbf{x}_n) \end{bmatrix}.$$

Many functions can be used as a correlation function[15, 31]. In this paper, the cubic spline function is used as the correlation function $\rho(\mathbf{x}_i, \mathbf{x}_j)$,

$$\rho(\mathbf{x}_i, \mathbf{x}_j) = \begin{cases} \frac{2}{3} - 4r_{ij}^2 + 4r_{ij}^3, & r_{ij} \leq \frac{1}{2}, \\ \frac{4}{3} - 4r_{ij} + 4r_{ij}^2 - \frac{4}{3}r_{ij}^3, & \frac{1}{2} < r_{ij} \leq \frac{1}{2}, \\ 0, & r_{ij} > 1, \end{cases}$$

where $r_{ij} = \frac{\|\mathbf{x}_i - \mathbf{x}_j\|}{\delta_i}$ and δ_i is the support size of node i . It should be noted that the shape function of the MKI possesses the Kronecker delta function property. This property enables meshless methods to impose the Dirichlet boundary condition directly.

The first-order partial derivatives of $u^h(\mathbf{x})$ with respect to $\mathbf{x} = (x, y)$ can be easily obtained from (8)-(9) as

$$u_{,k}^h(\mathbf{x}) = \Phi_{,k}(\mathbf{x})\mathbf{u},$$

$$\Phi_{,k}(\mathbf{x}) = \mathbf{p}_{,k}(\mathbf{x})\mathcal{A} + \mathbf{r}_{,k}(\mathbf{x})\mathcal{B},$$

where $(\cdot)_{,k}$ denotes $\partial(\cdot)/\partial x$ or $\partial(\cdot)/\partial y$.

3.2 Modification of correlation function

Consider a domain with two different materials separated by the interface Γ that splits all nodes into two sets: Λ^+ and Λ^- , where Λ^+ (Λ^-) contains all the indexes of nodes that belong exclusively to region $\bar{\Omega}^+$ ($\bar{\Omega}^-$).

For the modification of the correlation function, the following procedure is considered:

$$\rho^\pm(\mathbf{x}_i, \mathbf{x}_j) = \begin{cases} \rho(\mathbf{x}_i, \mathbf{x}_j), & i, j \in \Lambda^\pm, \\ 0, & \text{otherwise.} \end{cases}$$

Using the modification of correlation function, the approximation u^h to the u is then given by

$$u^h(\mathbf{x}) = u^{h\pm}(\mathbf{x}), \quad \mathbf{x} \in \bar{\Omega}^\pm,$$

where

$$u^{h+}(\mathbf{x}) = \sum_{i \in \Lambda^+} \phi_i^+(\mathbf{x}) u_i^+,$$

$$u^{h-}(\mathbf{x}) = \sum_{i \in \Lambda^-} \phi_i^-(\mathbf{x}) u_i^-.$$

3.3 Derivation of the discretized equations

Now, we will seek a discrete solution u^h in the finite-dimensional space \mathcal{U}^h such that

$$a(u^h, v^h) = l(v^h), \quad \forall v^h \in \mathcal{V}^h,$$

where $\mathcal{U}^h \subset \mathcal{U}$ and $\mathcal{V}^h \subset \mathcal{V}$. Substituting MKI shape function for trial and test functions into (6)-(7), a linear algebraic system is obtained that can be written in the form:

$$\begin{bmatrix} A^- & B \\ B^T & A^+ \end{bmatrix} \begin{bmatrix} \mathbf{u}^- \\ \mathbf{u}^+ \end{bmatrix} = \begin{bmatrix} \mathbf{f}^- \\ \mathbf{f}^+ \end{bmatrix},$$

where

$$A_{ij}^\pm = \int_{\Omega^\pm} (\kappa^\pm \nabla \phi_j^\pm \cdot \nabla \phi_i^\pm + \beta^\pm \phi_j^\pm \phi_i^\pm) d\Omega$$

$$\pm \frac{1}{2} \int_{\Gamma} (-\kappa^\pm \nabla \phi_j^\pm \cdot \mathbf{n} \phi_i^\pm - \phi_j^\pm \kappa^\pm \nabla \phi_i^\pm \cdot \mathbf{n} + 2\alpha \phi_j^\pm \phi_j^\pm) ds,$$

$$B_{ij} = \frac{1}{2} \int_{\Gamma} (\phi_i^+ \kappa^- \nabla \phi_j^- \cdot \mathbf{n} + \kappa^+ \nabla \phi_i^+ \cdot \mathbf{n} \phi_j^- - 2\alpha \phi_i^+ \phi_j^-) ds,$$

$$f_i^\pm = \int_{\Omega^\pm} f^\pm \phi_i^\pm d\Omega + \int_{\partial\Omega_N} g_N \phi_i^\pm ds \\ + \frac{1}{2} \int_{\Gamma} (\pm 2\alpha \phi_i^\pm g_1 - \kappa^\pm \nabla \phi_i^\pm \cdot \mathbf{n} g_1 + \phi_i^\pm g_2) ds,$$

$$\mathbf{u}^\pm = [u_1^\pm, u_2^\pm, \dots, u_{N_{\Lambda^\pm}}^\pm]^T.$$

4 Numerical results

In this section, some numerical results are presented to demonstrate the efficiency and accuracy of the proposed method. The numerical errors of computations are measured in two discrete norms L_∞ and L_2 . For all test examples, the computational domain Ω is the square $(x, y) \in [-1, 1] \times [-1, 1]$ and the interface Γ is represented by a circle with center at the origin and radius $r_0 = \frac{1}{2}$. To construct nodal distribution for studied geometry with both uniformly and nonuniformly distributed, the strategy expressed in [28] is intended. In this work, h is the distance between points in the domain Ω where the solution is approximated in a uniformly distributed mesh. The integration of the global weak form is carried out numerically by a Gaussian quadrature [4, 10, 22]. The shifted and scaled quadratic polynomial basis functions are used to stabilize the MKI scheme [31] where a quadratic polynomial basis is considered. In the first four examples, the Dirichlet boundary condition is considered as a boundary condition while in the last example, the mixed boundary condition will be studied. In all of the studied examples, the Dirichlet boundary condition and the jump conditions are computed according to the given exact solution.

Example 1. As the first example, the Laplace equation $\nabla^2 u(x, y) = 0$ is considered. This equation is solved with the nonhomogeneous jump in the solution and its flux across the interface. The exact solution is given

$$(u^+(x, y), u^-(x, y)) = (0, \exp(x) \cos(y)).$$

Table 1 shows the obtained error by the proposed technique. The numerical error in terms of L_∞ -norm and L_2 -norm is represented.

Table 1: The values of error in Example 1.

h	0.2	0.1	0.05	0.025	0.0125
L_∞ -norm	6.31e-3	1.57e-3	4.78e-4	1.52e-4	5.10e-5
L_2 - norm	3.15e-3	9.34e-4	3.91e-4	9.25e-5	3.93e-5

Example 2. In this example, the Poisson interface problem is studied with the homogeneous jump in the solution and its flux across the interface. The equation $\nabla \cdot (\kappa \nabla u(x, y)) = 9\sqrt{x^2 + y^2}$ is considered with the discontinuous coefficient κ . The exact solution is

$$(u^+(x, y), u^-(x, y)) = \left(\frac{(x^2 + y^2)^{3/2}}{\kappa^+} + \frac{1}{8} \left(\frac{1}{\kappa^-} - \frac{1}{\kappa^+} \right), \frac{(x^2 + y^2)^{3/2}}{\kappa^-} \right).$$

Table 2 reports the behavior of the approximation error with large jump in the κ coefficient. The numerical errors in terms of L_2 -norm and L_∞ -norm are collected for $(\kappa^+, \kappa^-) = (1000, 1)$. Also, the numerical results using the proposed method have been compared with the obtained results in [18].

Table 2: The values of error in Example 2.

h	0.2	0.1	0.05	0.025	0.0125
L_∞ -norm	3.12e-3	9.61e-4	5.31e-4	1.91e-4	6.42e-5
L_2 - norm	2.72e-3	7.81e-4	2.63e-4	7.19e-5	2.60e-5
L_∞ - norm [18]	3.71e-3	2.77e-3	1.71e-3	1.09e-3	4.68e-4
L_2 - norm[18]	2.03e-3	9.58e-4	3.95e-4	1.26e-4	3.68e-5

Example 3. To study the Poisson interface problem with a nonhomogenous jump in the solution and its flux across the interface, this example is considered. Consider $\nabla \cdot (\kappa \nabla u(x, y)) = f(x, y)$, where κ and f are discontinuous across the interface. The exact solution to the equation, the coefficient κ , and the source term f of the equation are given as follow

$$(u^+(x, y), u^-(x, y)) = \left(\frac{1}{4} \left(1 - \frac{1}{80} - \frac{1}{10} \right) + \left(\frac{(x^2 + y^2)^2}{2} + x^2 + y^2 \right) / 10, x^2 + y^2 - 1 \right),$$

$$(\kappa^+, \kappa^-) = (10, 2), \quad (f^+(x, y), f^-(x, y)) = (8(x^2 + y^2) + 4, 8).$$

In Table 3, the refinement of the proposed method at different values of mesh sizes is observed.

Table 3: The values of error in Example 3.

h	0.2	0.1	0.05	0.025	0.0125
L_∞ -norm	6.31e-3	1.67e-3	5.01e-4	1.28e-4	6.27e-5
L_2 - norm	1.92e-3	6.29e-4	1.64e-4	4.52e-5	1.14e-5

Example 4. In this example, the behavior of the proposed method for the Helmholtz equation with discontinuous coefficients κ and β is studied. Consider $\nabla \cdot (\kappa \nabla u(x, y)) + \beta u(x, y) = f(x, y)$, where the discontinuous coefficients κ and β are

$$(\kappa^+, \kappa^-) = (10, 1), \quad (\beta^+, \beta^-) = (40, 4).$$

The exact solution to the equation is as follows

$$(u^+(x, y), u^-(x, y)) = (\sin(2x) \cos(2y), x^2 + y^2).$$

The values of error are reported in Table 4. Also, the achieved errors are compared with the obtained numerical results in [18].

Table 4: The values of error in Example 4.

h	0.2	0.1	0.05	0.025	0.0125
L_∞ -norm	9.06e-2	1.22e-2	8.65e-3	8.54e-3	2.13e-3
L_2 - norm	7.59e-2	9.01e-3	5.19e-3	1.33e-3	1.87e-3
L_∞ - norm [18]	1.27e-1	4.74e-2	5.04e-2	5.50e-3	3.80e-3
L_2 - norm[18]	9.63e-2	5.61e-2	1.49e-2	2.40e-3	1.50e-3

Example 5. Consider the Poisson interface problem $\nabla \cdot (\kappa \nabla u(x, y)) = f(x, y)$ where the κ coefficient and term source f are chosen to be

$$(\kappa^+, \kappa^-) = (1, 2), \quad (f^+, f^-) = (4, -4 \sin(x) \sin(y)).$$

The exact solution is

$$(u^+, u^-) = (x^2 + y^2, \sin(x) \sin(y)).$$

The boundary conditions are considered as follows

$$\begin{aligned} \frac{\partial u}{\partial x}(-1, y) &= -2, & y \in [-1, 1], \\ \frac{\partial u}{\partial y}(x, -1) &= -2, & x \in [-1, 1], \\ u(1, y) &= 1 + y^2, & y \in [-1, 1], \\ u(x, 1) &= 1 + x^2, & x \in [-1, 1]. \end{aligned}$$

In this example, the interface problem is solved with regularly and irregularly distributed nodes. Table 5 presents the achieved errors of both node distributions.

Table 5: The values of error in Example 5.

$(N_{\Lambda+}, N_{\Lambda-})$	(425, 132)	(1393, 389)	(5473, 1433)	(21219, 5411)
$L_{\infty} - norm\{\text{regular}\}$	6.15e-2	2.17e-2	9.77e-3	6.02e-3
$L_{\infty} - norm\{\text{irregular}\}$	9.13e-2	5.49e-2	2.37e-2	8.73e-3

5 Conclusion

In this work, an efficient element free Galerkin scheme was proposed for solving the second-order elliptic interface problems with homogeneous and nonhomogeneous jump conditions. In the proposed method, the shape functions were built by the moving kriging interpolation scheme which has the Kronecker delta property. Therefore, the Dirichlet boundary condition was imposed directly and easily. The modification of the correlation function was used in a very simple and effective way of creating the appropriate discontinuous shape functions. To weakly enforce the jump condition, a variational consistent Nitsche type method was used. In all five studied examples, the numerical results showed the efficiency and accuracy of the proposed method for the studied elliptic interface problems.

References

- [1] M. Ahmad, S.U. Islam and E. Larsson, Local meshless methods for second order elliptic interface problems with sharp corners, *Journal of Computational Physics*, 416 (2020) 109500.
- [2] N. R. Aluru and G. Li, Finite cloud method: a true meshless technique based on a fixed reproducing kernel approximation, *International Journal for Numerical Methods in Engineering*, 50 (2001), 2373-2410.

- [3] S.N. Atluri and T. Zhu, A new meshless local Petrov-Galerkin (MLPG) approach in computational mechanics, *Computational Mechanics*, 22 (1998), 117-127.
- [4] I. Babuska, U. Banerjee, J. E. Osborn, Q. Zhang, Effect of numerical integration on meshless methods, *Computer Methods in Applied Mechanics and Engineering*, 198 (2009), 2886-2897.
- [5] T. Belytschko and M. Fleming, Smoothing, enrichment and contact in the element-free Galerkin method, *Computers & Structures*, 71 (1999), 173-195.
- [6] T. Belytschko, Y. Lu and L. Gu, Element free Galerkin methods, *International Journal for Numerical Methods in Engineering*, 37 (1994), 229-256.
- [7] L.W. Cordes and B. Moran, Treatment of material discontinuity in the element-free Galerkin method, *Computer Methods in Applied Mechanics and Engineering*, 139 (1996), 75-89.
- [8] M. Dehghan and M. Abbaszadeh, Interpolating stabilized moving least squares (MLS) approximation for 2D elliptic interface problems, *Computer Methods in Applied Mechanics and Engineering*, 328 (2018), 775-803.
- [9] M. Dehghan and M. Abbaszadeh, Two meshless procedures:moving Kriging interpolation and element-free Galerkin for fractional PDEs, *Applicable Analysis*, 96 (2017), 936-969.
- [10] M. Dehghan, M.R. Eslahchi, Best uniform polynomial approximation of some rational functions, *Computers and Mathematics with Applications*, 59 (2010) 382-390.
- [11] J. Dolbow and T. Belytschko, An introduction to programming the meshless element free Galerkin method, *Archives of Computational Methods in Engineering*, 5 (1998), 207-241.
- [12] J. Dolbow and I. Harari, An efficient finite element method for embedded interface problems, *International Journal for Numerical Methods in Engineering*, 78 (2009), 229-252.

- [13] T.P. Fries, T. Belytschko, The extended/generalized finite element method: An overview of the method and its applications, *International Journal for Numerical Methods in Engineering*, 84 (2010), 253-304.
- [14] F. Gholampour, E. Hesameddini and A.Taleei, A global RBF-QR collocation technique for solving two-dimensional elliptic problems involving arbitrary interface, *Engineering with Computers*, (2020). <https://doi.org/10.1007/s00366-020-01013-y>.
- [15] L. Gu, Moving kriging interpolation and element-free Galerkin method, *International Journal for Numerical Methods in Engineering*, 56 (2003), 1-11.
- [16] A. Hansbo and P. Hansbo, An unfitted finite element method, based on Nitsche's method, for elliptic interface problems, *Computer Methods in Applied Mechanics and Engineering*, 191 (2002), 5537-5552.
- [17] S.U. Islam and M. Ahmad Meshless analysis of elliptic interface boundary value problems, *Engineering Analysis with Boundary Elements*, 92 (2018), 38-49.
- [18] Z. Jannesari and M. Tatari, Element free Galerkin method to the interface problems with application in electrostatic, *International Journal of Numerical Modelling: Electronic Networks, Devices and Fields*, 29 (2016), 1089-1105.
- [19] P. Krysl and T. Belytschko, Element-free Galerkin: convergence of the continuous and discontinuous shape functions, *Computer Methods in Applied Mechanics and Engineering*, 148 (1997), 257-277.
- [20] X. Li and H. Dong, Error analysis of the meshless finite point method, *Applied Mathematics and Computation*, 382 (2020), 125326.
- [21] Z. Li and K. Ito, *The Immersed Interface Method: Numerical Solutions of PDEs Involving Interfaces and Irregular Domains*, SIAM Frontier in Applied Mathematics (2006).

- [22] M. Masjed-Jamei, M.R. Eslahchi, M. Dehghan, On numerical improvement of Gauss-Radau quadrature rules, *Applied Mathematics and Computation*, 168 (2005), 51-64.
- [23] Y. Mukherjee and S. Mukherjee, On boundary conditions in the element-free Galerkin method, *Computational Mechanics*, 19 (1997), 264-270.
- [24] V.P. Nguyen, T. Rabczuk, S. Bordas and M. Duflot, Meshless methods: A review and computer implementation aspects, *Mathematics and Computers in Simulation*, 79 (2008), 763-813.
- [25] S. Samimi and A. Pak, A novell three-dimensional element free Galerkin (EFG) code for simulating two-phase fluid flow in porous materials, *Engineering Analysis with Boundary Elements*, 39 (2014), 53-63.
- [26] R. Salehi and M. Dehghan, A generalized moving least square reproducing kernel method, *Journal of Computational and Applied Mathematics*, 249 (2013), 120-132.
- [27] G. R. Rohit, J. M. Prajapati and V. B. Patel, Coupling of Finite Element and Meshfree Method for Structure Mechanics Application: A Review, *International Journal of Computational Methods*, 17 (2020), 1850151.
- [28] A. Taleei and M. Dehghan, Direct meshless local Petrov-Galerkin method for elliptic interface problems with applications in electrostatic and elastostatic, *Computer Methods in Applied Mechanics and Engineering*, 278 (2014), 479-498.
- [29] A. Taleei and M. Dehghan, An efficient meshfree point collocation moving least squares method to solve the interface problems with nonhomogeneous jump conditions, *Numerical Methods for Partial Differential Equations*, 31 (2015), 1031-1053.
- [30] A. Taleei, A moving kriging interpolation-based meshfree method for solving two-phase elasticity system, *Journal of Mathematical Modeling*, 9 (2021) 1-12.

- [31] S. Tu, H. Yang, L.L. Dong and Y. Huang, A stabilized moving Kriging interpolation method and its application in boundary node boundary, *Engineering Analysis with Boundary Elements*, 100 (2019), 14-23.
- [32] R. Vaghefi, Three-dimensional temperature-dependent thermo-elastoplastic bending analysis of functionally graded skew plates using a novel meshless approach, *Aerospace Science and Technology*, 104 (2020), 105916.
- [33] J. Wang and F. Sun, A hybrid generalized interpolated element-free Galerkin method for Stokes problems, *Engineering Analysis with Boundary Elements*, 111 (2020), 88-100.
- [34] F. Wang, G. Lin, Y. Zhou and D. Chen, Element-free Galerkin scaled boundary method based on moving Kriging interpolation for steady heat conduction analysis, *Engineering Analysis with Boundary Elements*, 106 (2019), 440-451.
- [35] Y. Xing, L. Song, X. He and C. Qiu, The generalized finite difference method for solving elliptic interface problems, *Mathematics and Computers in Simulation*, 178 (2020), 109-124.

Ameneh Taleei

Assistant Professor of Mathematics

Department of Mathematics

Shiraz University of Technology

Shiraz, Iran

E-mail: a.taleei@sutech.ac.ir